Comparison of different control strategies for series-series compensated inductive power transmission systems

J. Tritschler*, B.Goeldi*, S.Reichert*, G.Griepentrog°
*Fraunhofer Institute for Solar Energy Systems, Freiburg
°Institute for Power Electronics and Control of Drives, TU Darmstadt
Germany
Johannes.tritschler@ise.fraunhofer.de
http://www.ise.fraunhofer.de

Keywords

«Wireless power transmission», «Efficiency», «Contactless Energy Transfer», «Battery Charger», «Automotive Electronics»

Abstract

For automotive battery charging, the series-series compensated inductive power transmission shows a lot of advantages compared to other compensation techniques. As shown in many recent [1], [2] and older publications, the main advantages are the independency of the secondary current from the load at resonant frequency and the zero phase shift between primary current and voltage. As shown in [3], very high efficiencies from grid to battery of nearly 94-95% can be reached by driving the IPT-system at constant frequency and by adapting the input and the output DC-link voltages. To achieve this control method, extra DC/DC-converters need to be added inside the power transmission path. To avoid the thereby associated higher hardware and also software effort, alternative control strategies needing fewer components are of major interest.

In this paper, different control strategies and modulation schemes with and without additional DC/DC-converters are presented, theoretically evaluated with a special emphasis on partial load transmission efficiency and a selection is measured in a real system. The various control strategies were compared on one single coil geometry. The aim is to find a control method which minimizes the total system costs and maximizes the system efficiency at the same time.

Introduction

Depending on the battery-type of an electric vehicle, most of the time the car will be charged at full power. Only in the end of the charging process the charging current has to be reduced. Thus, concerning the charging efficiency of EV-battery chargers, particularly the full power operation point should have an excellent performance.

In the case of inductive power transmission systems, the applied control strategy plays an outstanding role, as it determines the system efficiency at both: partial-load, but even more important at full-load and when the two coils are misaligned. This circumstance will be explained in the following.

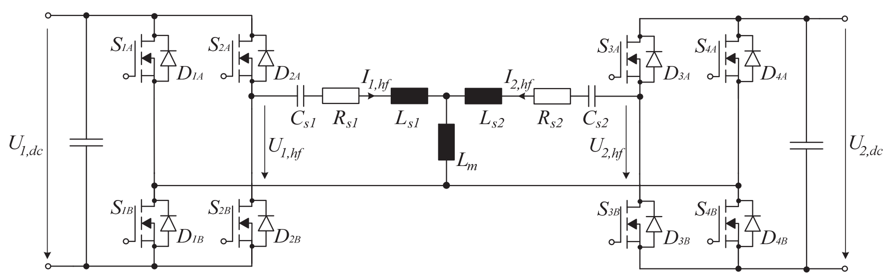

Figure 1: Series-Series compensated inductive power transmission system

As already mentioned, a series-series compensated system (Figure 1) was chosen, as it is expected to reach the highest efficiencies due to the absence of reactive currents between the coils and the resonant capacitors.
To achieve a load independency of the secondary current and to avoid reactive power, the self-inductance which is the sum of the leakage and main inductance (**L_s** and **L_m**) will be compensated:

$$f_0 = \frac{1}{2\pi\sqrt{(L_s + L_m) \cdot C_s}}$$

When driving the circuit at the resonant frequency **f_0**, the T-equivalent circuit (Figure 2) with the load resistance **R_L** can be derived.

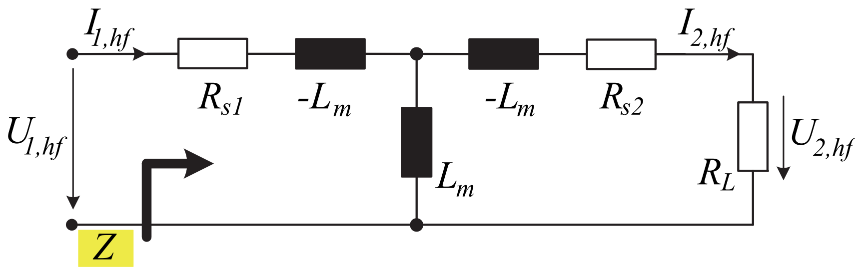

Figure 2: T-equivalent circuit at resonance with resistive load

The dependency between the fundamental of the secondary current **$I_{2,hf}(\omega_0)$** and the primary voltage **$U_{1,hf}(\omega_0)$** can be expressed via the mutual inductance by neglecting the copper resistances **R_{s1}** and **R_{s2}**:

$$|\boldsymbol{I_{2,hf}(\omega_0)}| = \frac{|\boldsymbol{U_{1,hf}(\omega_0)}|}{\boldsymbol{L_m \omega_0}}$$

Normally, the system should be designed to deliver full power at nominal coil positioning and minimum battery voltage.
Assuming the coils are misaligned, the mutual inductance **L_m** will be smaller compared to the nominal positioning. Considering the dependency between **$I_{2,hf}$** and **$U_{1,hf}$**, this leads automatically to a higher current **$I_{2,hf}$** if **$U_{1,hf}$** is kept constant. In order to not exceed the maximum power rating, the secondary current needs to be controlled by changing **$U_{1,hf}$** or by applying other control strategies. It's not possible anymore to drive the primary H-Bridge in normal operation mode. That's the main reason, why the control strategies in inductive power transmission systems for EVs play a very important role.

Control via DC/DC-converters

One possibility to control the power flow is to add extra DC/DC-converters. They can be on one or on both sides. It was shown in [3], [4] that very high efficiencies through the whole transmission path from grid to battery can be reached, when using two DC/DC converters (Figure 3).

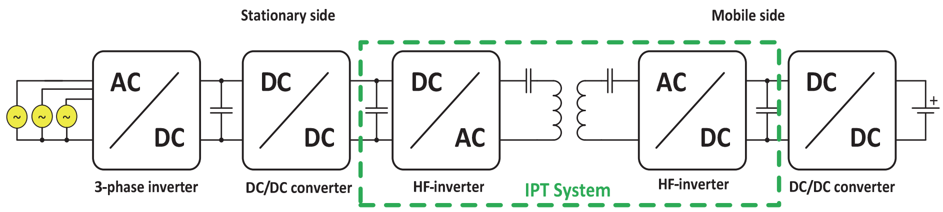

Figure 3: IPT-system from grid to battery with extra DC/DC-converters

This solution leads to very low losses inside the IPT-system, what could be very useful for some high power applications needing passive cooling. The main drawback of this system topology is the very high hardware effort (e.g. semiconductors, chokes, gate drivers) and software efforts and finally high costs. The only reasonable usage of this system configuration is, when the mobile power electronics have a dual use purpose as conductive and inductive charging system at the same time. In this case, the shown topology has real advantages compared to others.

Analysis of the system behavior

Mostly, only the fundamental analysis of the IPT system (Figure 1) is done. This is sufficient for nominal operation points and to define the maximum current and voltage ratings. But to truly understand the system behavior for different coupling and operating conditions and to estimate the system performance such as switching losses, a more detailed analysis has to be done. An investigation of the harmonics [5] is needed to mathematically describe the voltage and current waveforms.

First, the time signals of the primary and secondary voltages are transferred into the frequency domain and then the corresponding currents are calculated, summed up and finally transferred back to the time domain (Figure 4).

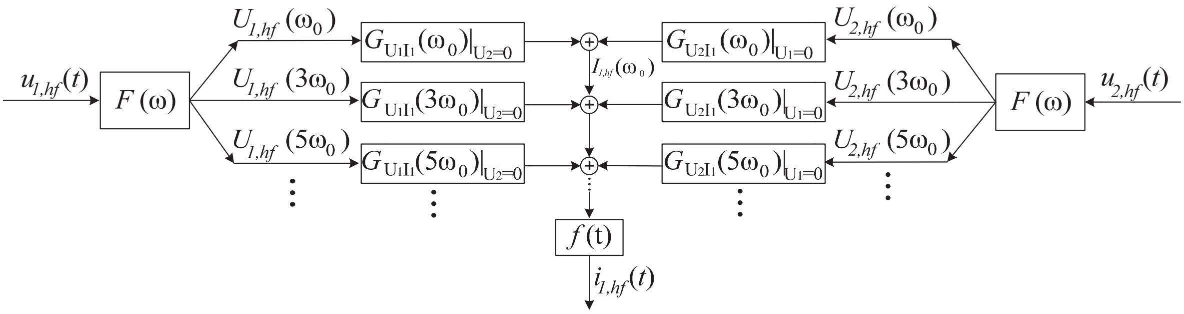

Figure 4: Description of the analytical calculations to investigate the system behavior

As far as the input voltages $u_{1,hf}(t)$ and $u_{2,hf}(t)$ are known and have the characteristic of periodic signals, the current waveforms for different control strategies can be calculated and evaluated. The considered system has a rated power of 11 kW. The main inductance has a value of L_m=27 µH and the self-inductance a value of L_1=68 µH. In Figure 5 , the calculated and measured current and voltage waveforms for $U_{1,hf}$=650 V and $U_{2,hf}$=300 V can be seen. The operating frequency is set to 90 kHz.

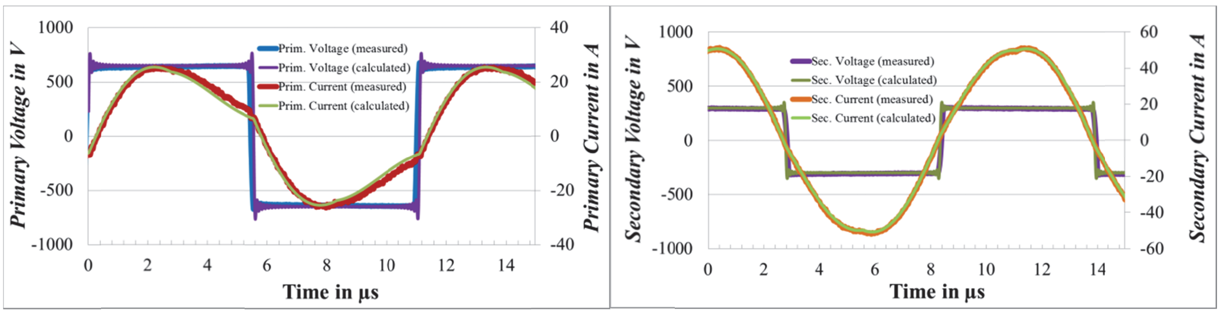

Figure 5: Calculated and measured current and voltage waveforms

As one can see, the calculation and the measurements match very well. The reason for the small phase delay between calculated and measured secondary voltages is due to the commutation of the rectifier diodes which was neglected in the calculations. The described method is used in the following to estimate and understand the system performance for different control strategies without DC/DC-converters. The investigated control strategies are:

- Phase shifted modulation (PSM)
- Pulse density modulation (PDM)

Primary Phase shifted control

The phase shifted control is well known from the phase-shifted-fullbridge topology of DC/DC-converters. The both legs of the primary fullbridge are driven with a constant duty cycle D of 0.5 and the signals of the first leg are phase shifted relatively to the signals of the second leg. The resulting primary voltage has a certain effective duty cycle which is proportional to the phase shift angle. For switching ON, ZVS is achieved but the switching OFF still produces switching losses. The primary current of the system mostly depends on the secondary voltage, so changing the primary voltage doesn't have a big impact on the height of the primary current. The conduction losses on the primary nearly stay the same, independently of the effective duty cycle, but the switching losses increase very fast, when the transferred power gets smaller. The principle doesn't change when this control method is applied on the secondary side. The partial load efficiency will be very poor in both cases [6].

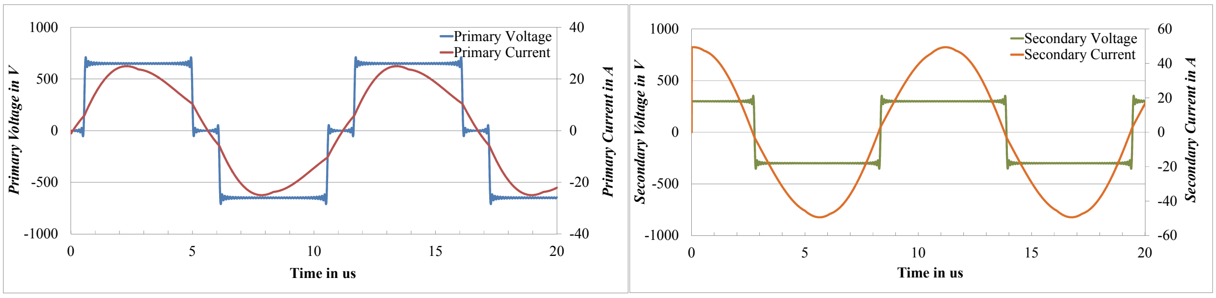

Figure 6: Calculated Waveforms for D=0.8

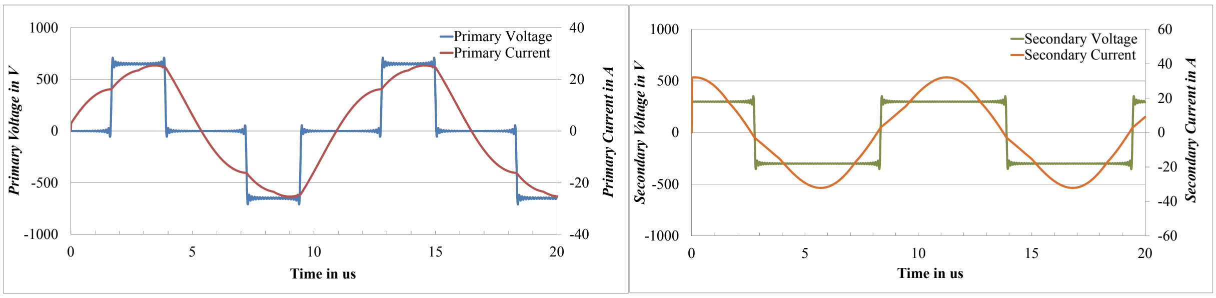

Figure 7: Calculated Waveforms for D=0.4

The height of the primary current during the transition from zero volts to positive or negative voltages determines the switching losses. The switched currents for the two legs of the full bridge are different, caused by the harmonic distortion of the current waveforms (Figure 8).

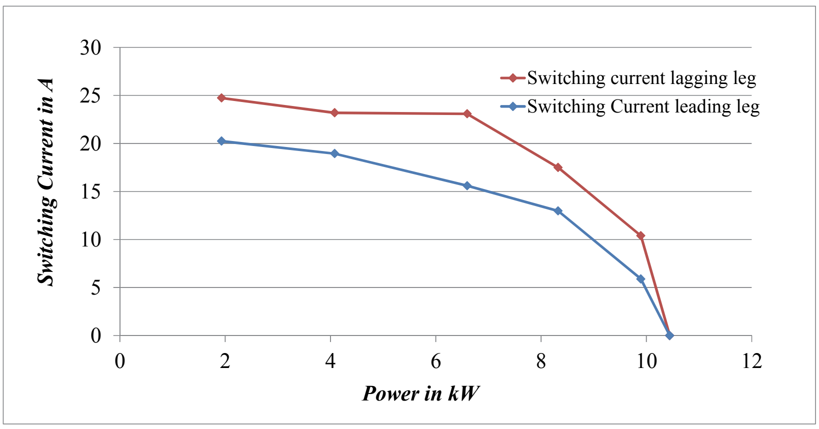

Figure 8: Current at switching events

To decrease the system losses, a dual control method can be applied which controls the input voltages on both sides, the primary and the secondary. This requires additional active switches and control mechanisms on the secondary side.

Pulse density modulation (PDM)

The pulse density modulation technique is well known from induction heating processes. The main advantage of this control strategy is its capability to keep the switching losses at a nearly constant level for a wide power range. It controls the power flow by shortening the primary side for a multiple of the resonant period T_0 (Figure 9) [7]. The primary current (blue) then circulates in the primary resonant tank and on the secondary side the rectifier will block the secondary current (green), as the induced voltage (purple) is lower than the DC-link voltage. In a next step, energy will be transferred from the primary side to the secondary side for a multiple of T_0.

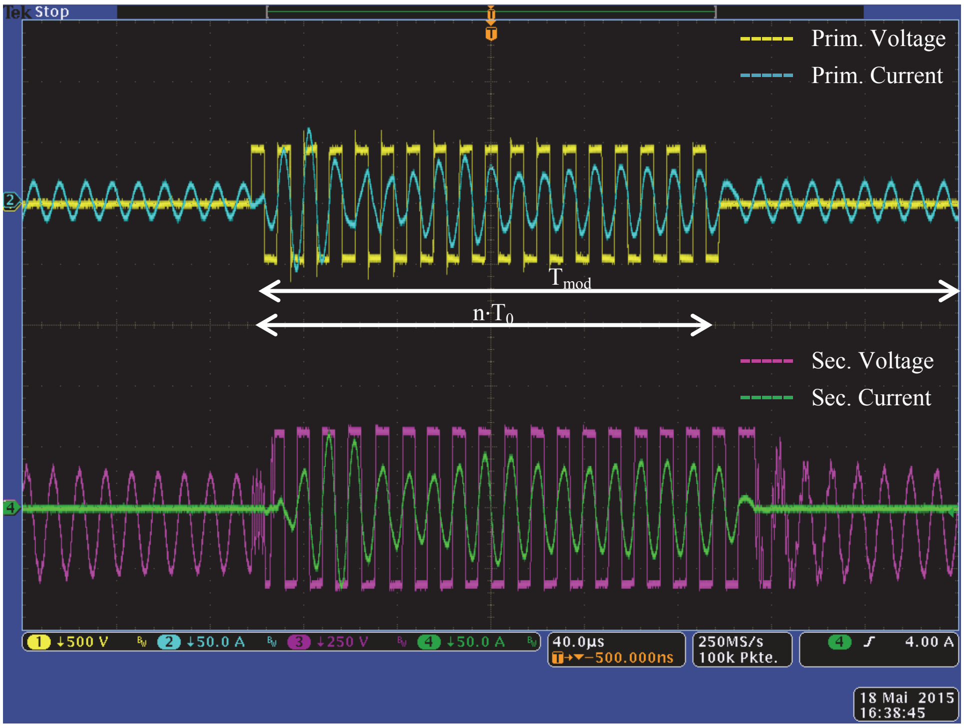

Figure 9: Full-bridge PDM

As one can see, the current and voltage on the primary side are mostly in phase which results in very low switching losses. By using the mathematical analysis previously presented, the harmonics can be calculated and are visualized in Figure 10.

At conventional full power operation, only the fundamental of the resonant frequency f_0=90 kHz and the 3^{rd}, 5^{th},… harmonics would appear in the Fourier spectrum. As shown in [7] the primary and secondary currents are nearly independently of the voltages on the same sides (see also Figure 6, Figure 7). The reason for this is that all the other frequency components except the fundamental frequency $\mathbf{f_0}$ are damped very well.

Contrary to that, in the case of PDM waveforms, especially the harmonics of the primary voltage (Figure 10) around the resonant frequency f_0=90 kHz are quite high. This results in relatively high non resonant frequency components in the current waveforms. The result of this is that the current waveforms show a low frequency modulation which results in higher maximum current values. Nevertheless, the r.m.s.-value of the currents for the period T_{mod} are not higher than for other controls strategies, so that the semiconductors don't need to handle more continuous current with the PDM control mechanism.

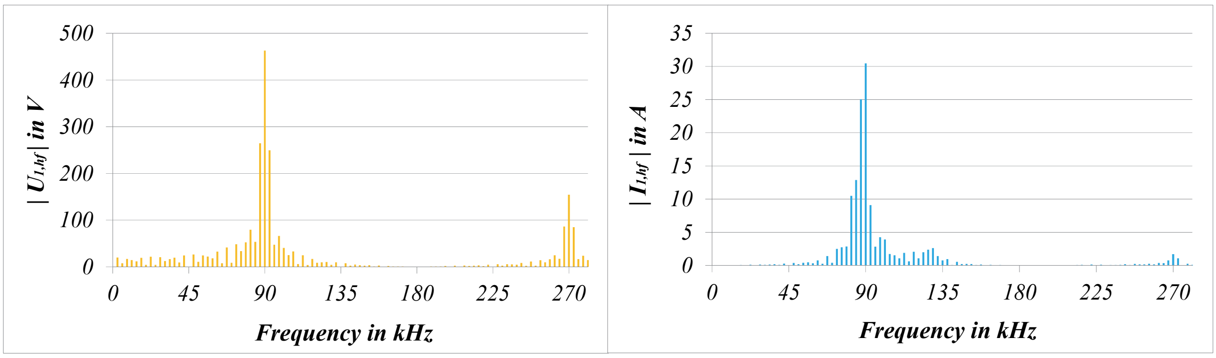

Figure 10: Harmonics of the primary voltage and current

When the time period of power transfer and the time period of circulating currents are identical ($n \cdot T_0 = T_{mod}/2$), approximately half of the full power will be transferred to the secondary side. In this case, for a power less than half of the full power, it could be useful to use the primary full-bridge only in half bridge mode (Figure 11). This increases the efficiency significantly, as the switching losses are lowered.

Figure 11: Half-bridge PDM

As the power transfer is pulsating, with a lower frequency than the resonant frequency, the DC-link capacitors need to be increased in order not to exceed the allowable voltage ripple. It can also happen that the circuit will produce an audible noise. This phenomenon can be avoided by choosing appropriate components so that the noise will not occur anymore.

Experimental Comparison

The different control strategies were compared in open loop. The used hardware is built up as an 11 kW system. To reduce the primary switching losses, SiC MOSFETs C2M0025120D were used together with passive rectifier diodes (C5D50065D) on the secondary side.

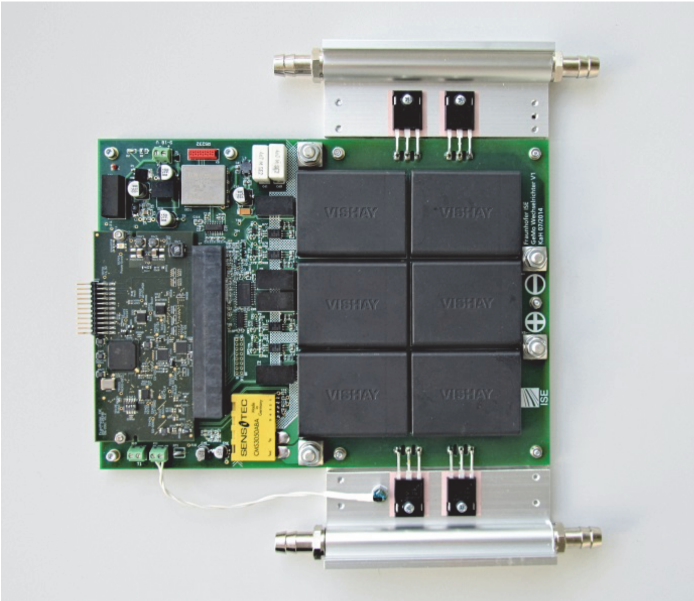

Figure 12: Prototype of primary side inverter

A lab prototype was developed and is shown in Figure 12. The primary and secondary hardware are very flat in order to have the opportunity to assemble the coils and the power electronics together in a flat housing.
The measured efficiencies of the different control strategies are done in open loop and were presented in Figure 13. The primary voltage is set to 650 V and the secondary voltage to 300 V.

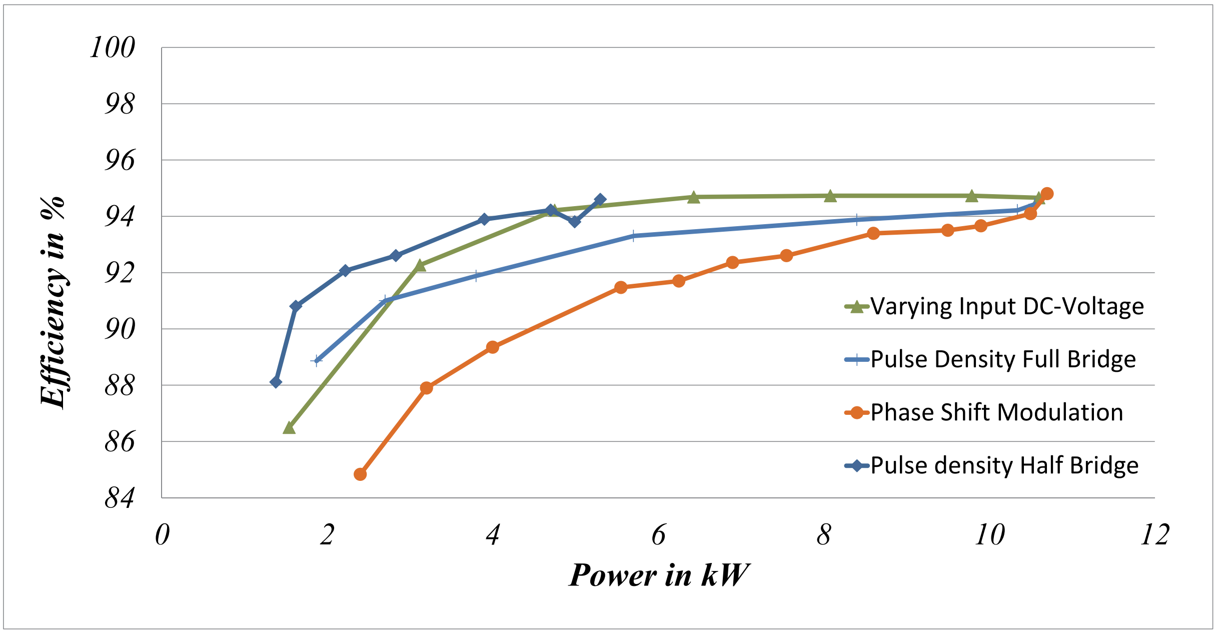

Figure 13: Measurement results

The phase-shift-modulation (orange) has a very poor efficiency at partial load, as it produces more and more switching losses with less power transferred. The increase in efficiency when using a half bridge pulse density modulation compared to the full-bridge pulse density modulation is up to 2 percentage points. At partial load, it’s even better than the efficiency with varying input voltages. It has to be considered, that the efficiency measurement of the varying input voltages doesn’t include the therefore needed DC/DC-converter. Even assuming a very good efficiency of the DC/DC-converter, the overall efficiency would be the same as, or lower, than that achieved with pulse density modulation.

Conclusion

Three control strategies have been experimentally compared to each other. With the used hardware prototype it could be shown that the pulse density modulation is an excellent mechanism to achieve high efficiencies. They are even higher than the one reached with additional DC/DC-converter on both sides of the IPT . Combining the Full-bridge PDM and the half bridge PDM leads to a very low hardware effort and control complexity but a very high efficiency over a wide power range.

References

[1] B. Goeldi, S. Reichert, J. Tritschler: "Design and dimensioning of a highly efficient 22 kW bidirectional inductive charger for e-mobility", in Proc. Int. Exhibition and Conf. for Power Electronics (PCIM Europe), 2013, pp. 1496-1503

[2] Aditya K., Williamson S.S., "Comparative study of Series-Series and Series-Parallel compensation topologies for electric vehicle charging," Industrial Electronics (ISIE), 2014 IEEE 23rd International Symposium on , vol., no., pp.426,430, 1-4 June 2014

[3] B. Goeldi, J. Tritschler, S. Reichert: "Measurement Results of a 22 kW Bidirectional Inductive Charger", in Proc. Int. Exhibition and Conf. for Power Electronics (PCIM Europe), 2015

[4] Bosshard, R.; Kolar, J.W.; Wunsch, B., "Control method for Inductive Power Transfer with high partial-load efficiency and resonance tracking," Power Electronics Conference (IPEC-Hiroshima 2014 - ECCE-ASIA), 2014 International , vol., no., pp.2167,2174, 18-21 May 2014

[5] Voglitsis, D.; Todorcevic, T.; Prasanth, V.; Bauer, P., "Loss model and control stability of bidirectional LCL-IPT system," Electric Drives Production Conference (EDPC), 2014 4th International, pp.1, 2014

[6] Petersen, M.; Fuchs, F.W., "Load dependent power control in series-series compensated electric vehicle inductive power transfer systems," Power Electronics and Applications (EPE'14-ECCE Europe), 2014 16th European Conference on , vol., no., pp.1,10, 26-28 Aug. 2014

[7] Tritschler, J.; Reichert, S.; Goeldi, B., "A practical investigation of a high power, bidirectional charging system for electric vehicles," Power Electronics and Applications (EPE'14-ECCE Europe), 2014 16th European Conference on , pp.1,7, 26-28 Aug. 2014